OPTOELECTRONICS AND ADVANCED MATERIALS – RAPID COMMUNICATIONS Vol. 1, No. 9, September 2007, p. 417 - 424

# Optoelectronic properties of nanocrystalline F-doped $SnO_2$ (FTO) films prepared by sol-gel spin coating technique

N. SANKARASUBRAMANIAN, K. SANTHAKUMARI[a], V. S. VIDHYA[b], L. C. NEHRU[b], B. SUBRAMANIAN[b], A. THAYUMANAVAN[c], S. RAMAMURTHY[d], C. SANJEEVIRAJA[e], M. JAYACHANDRAN[b*]
*Department of Physics, Thiagarajar college of Engineering, Madurai-625015, India*
[a]*Department of physics, SASTRA University, Thirumalai Samuthiram-613402, India*
[b]*ECMS Division, Central Electrochemical Research Institute, Karaikudi-630006, India*
[c]*Department of Physics, AVVM Sri Pushpam College, Poondi-613503, India*
[d]*Department of Physics, Gandhigram Rural Institute, Gandhigram-624302, India*
[e]*Department of Physics, Alagappa University, Karaikudi-630003, India*

F-doped Transparent tin oxide thin films ($SnO_2$:F) have been prepared using the sol–gel spin coating technique. In order to optimize the dopant concentration, sol-gel samples of different F/Sn ratios from 1.0 to 12.5 at.%, were prepared, spin coated and heated at temperatures ranging from 325 to 450$^oC$ with an optimum number of 8 coatings. Their structural, optoelectronic and morphological properties were investigated. The X-ray diffraction (XRD) studies showed the nanocrystalline nature of the developed films. The films deposited at 400$^oC$ with a F/Sn ratio of 7.5 at.%, were highly transparent in the visible region with a refractive index value of about 2.0 and have low resistivity. Surface morphological studies by SEM and AFM images showed marked influence of F-dopant concentrations on the topography of $SnO_2$:F films.

(Received August 9, 2007; accepted August 31, 2007)

*Keywords*: Thin film, Spin coating, F doped tin oxide, Conducting oxide

## 1. Introduction

Tin oxide ($SnO_2$) film is an interesting and technologically important transparent conducting oxide (TCO) material which has shown potential applications in transparent conducting electrodes [1], solar cells [2], gas sensors [3], light emitting devices [4], white pigmented conductive paint coatings [5] and transparent heating film for ovens [6]. Many recent R&D efforts have been focused on the development of $SnO_2$ nano films like whiskers nanorods [7], nanowires [8], nanobelts [9] and naocrystalline/nanoporous films [10] to construct nanoscale electronic and optoelectronic devices [11]. Stoichimetric $SnO_2$ is an insulator. Electronic conduction in undoped tin oxide is due to the presence of oxygen vacancies, which contribute two electrons for conduction. $SnO_2$ crystallizes with tetragonal rutile structure with space group $D_{4h}^{14}$ [$P4_2/mnm$]. The unit cell contains uniquely positioned six atoms, two tin atoms and four oxygen atoms. Each tin atom is at the center of six oxygen atoms placed at the corners of a regular octahedron and every oxygen atom is surrounded by three tin atoms at the corners of an equilateral triangle facilitating easy doping with anions or cations or formation of point defects in native atoms.

It is well known that non-stoichiometric $SnO_2$ shows n-type conductivity with an electron concentration of more than $10^{20}$ $cm^{-3}$ which free carriers are generated by the following two mechanisms [12] of point defects in native atoms: (1) oxygen vacancies acting as electron donors, (2) ionization of tin interstitials giving rise to additional electron for conduction. Between these two mechanisms, the formation of carriers by oxygen vacancies has been accepted to be the predominant lattice carrier generation mechanism in intrinsic $SnO_2$ crystal. Further, an increase in the number of carriers in $SnO_2$ crystalline lattice may be effected by thermal treatment in hydrogen atmosphere [13] and by a suitabily selected doping element process [14]. In this aspect, much effort has been focused on the oxides of tin with small amount of other elements as dopants, e.g. antimony (Sb), fluorine (F) to impart higher conductivity, optical transmittance and chemical stability. The basic physics of tailoring such desirable properties results from the fact that this oxide having n-type band-gap between 3.0 to 3.7 eV and can be doped to give electron carriers in the conduction band. Substituting a monovalent $F^-$ anion for the divalent $O^{2-}$, a nearby tin atom is left with one excess electron which goes into the conduction band. F doping is advantageous and higher conductivity is realized in FTO crystalline lattice because of the higher carrier mobility observed due to the reduction in grain boundary scattering by anion doping rather than by cation doping. Hence, technologically fluorine doped tin oxide, $SnO_2$:F (FTO) has become an interesting n-type degenerate and wide band gap semiconductor which has been used in many devices due to its excellent conductivity, higher transparency in the visible region, mechanical and highly stable chemical properties [15].

FTO thin films can be prepared by many methods such as chemical vapour deposition (CVD) [16], photo CVD and thermal CVD [17], atmospheric pressure CVD [18], sputtering and thermal evaporation related methods and spray pyrolysis [19]. The properties of FTO films mainly depend on the method of preparation and growth parameters. However, chemical solution routes are considered very promising for depositing semiconductor oxide films due to their simplicity and low cost investment. Further, in view of technology requirements such as to prepare $SnO_2$:F films on electronic semiconductors and liquid-junction or organic solar cells containing organic materials, it is a prerequisite and compulsory to reduce the preparation temperature of oxide films below 500$^o$C. In this regard, recently an increasing interest towards the sol-gel synthesis of the $SnO_2$ based thin films [20-22] has been observed. It has inherent advantages such as increased capability to tailor complex compositions, simple and economical in technological equipment, low thermal budget necessary for oxide film consolidation and specific controlled porosity properties [21].

In the present work, the process of spin coating technique is optimized to prepare $SnO_2$:F films possessing nanocrystalline nature with good adherence, uniformity and stability using the sol-gel route. The structure, composition and optoelectronic properties of the FTO thin films depend on the fabrication parameters viz., nature of the sol, spin rate, spin time, dopant concentration, heat treatment temperature and number of coatings. It is necessary to optimize these coating parameters to get the best overall optoelectronic characteristics for the developed FTO films. To increase both the conductivity and stability of the films without altering the transparency, extraneous dopant, fluorine, is introduced into the lattice of tin oxide and a detailed study has been carried out to prepare FTO thin films by spin coating technique employing sol-gel route and their optoelectronic properties are presented here.

## 2. Experimental

### Preparation of sol

The sol was prepared with 0.37 M of tin chloride ($SnCl_4.5H_2O$) in 100 ml of ethyl alcohol. The desired amount of ammonium fluoride ($NH_4F$) was then added to the solution for fluorine (F) doping such that different F/Sn ratios of 1.0, 2.5, 5.0, 7.5, 10.0 and 12.5 at.% were maintained in the precursor sol. To increase the solubility of the solute and to induce simultaneous condensation and gelation, 5 ml of 0.1N concentrated hydrochloric acid was then added to the solution as a catalyst. The mixed solutions were stirred well and refluxed for about one hour at 60 °C. The solutions were cooled in the ambient and then aged in open beakers at room temperature, for gellation. After a period of 24 hr aging, the solution becomes increasingly cloudy and a gelatinous suspension, which homogeneously occupies the entire solution was subsequently formed. Fig. 1 shows the deposition procedure of $SnO_2$:F films by the sol-gel spin coating technique. A turn-table spin rate of 3000 rpm and a spin time of 10 seconds were used to coat the green sol-gel thin film on glass substrates. The sol-gel coated substrates were heated at a temperatures 300 $^o$C for 15 min in air after each spin-coating step whose thickness was about 45 nm for each coating. By repeating this step 8 times, pinhole free and uniform $SnO_2$:F films of thickness about 350 nm were obtained.

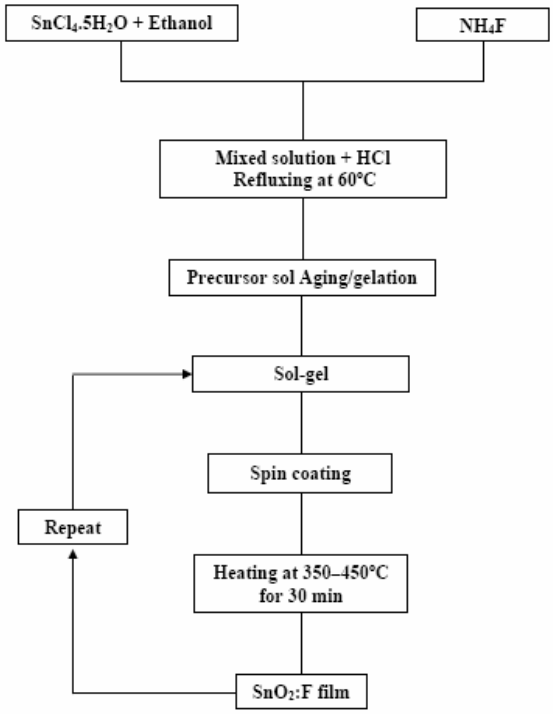


*Fig. 1. Deposition procedure for the sol-gel spin coating of $SnO_2$:F films.*

The prepared $SnO_2$ films have been characterised using JEOL JDX 803a X-ray diffractometer (XRD), Hitachi S3000H scanning electron microscope (SEM), and Nanoscope E scanning probe microscopy 3138J for atomic force microscopy (AFM) for structural, surface image and topography respectively. The optical transmission, electrical resistivity and carrier concentration measurements were carried out using Perkin Elmer Lambda 35 UV-Vis spectrophotometer, four probe resistivity instrument and Hall effect set-up respectively.

## 3. Results and discussion

### 3.1. Structural properties

#### *3.1.1 Optimization of heat treatment temperature*

XRD analysis of the FTO thin films spin coated and heated at temperatures 350, 375, 400, 425 and 450$^o$C keeping the number of coating as 8 and F/Sn ratio as 7.5 at.% was carried out and shown in Fig. 2. All the films

were polycrystalline and showed tetragonal rutile structure of tin oxide with preferred orientation along (110) plane. Other planes such as (101) and (211) are also observed with lower intensities and all are broad whose larger full width at half maximum (FWHM) is confirming the presence of nanocrystalline particles or aggregates in the films. The (110) peak shows the highest intensity in all the films heated at various temperatures range from 350 to 450 $^oC$. The sharpness and intensity of the orientations viz., (110), (101) and (211) increase as the heat treatment temperature is increased which reaches a maximum at 400 $^oC$ and then decreases gradually as the temperature is further raised to 450 $^oC$.

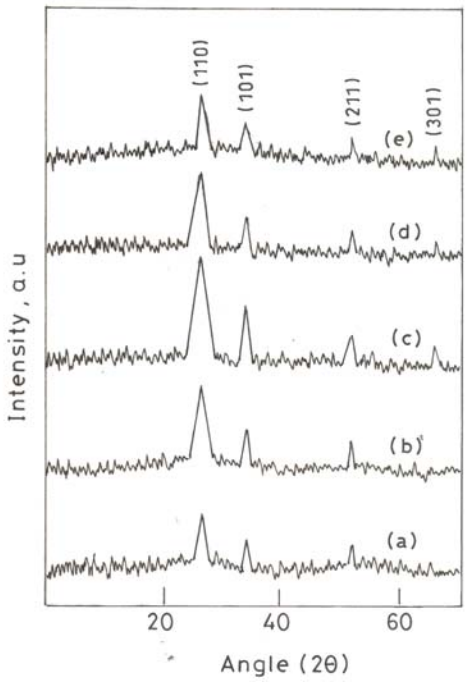


*Fig. 2. XRD pattern of 7.5% F doped $SnO_2$:F films heat treated at (a) 350, (b) 375, (c) 400, (d) 425 and (e) 450 $^oC$.*

At the optimum heat treatment temperature 400$^oC$, the lattice constant a, c and c/a ratio were calculated as 4.73A°, 3.19A° and 0.67, which are in agreement with the standard values of JCPDS data (41 – 1445) for $SnO_2$ powder specimen. The mean crystallite size increases from 4.3 nm to 6.9 nm for the films heat treated from 350 to 400 $^oC$ and then decreases to 4.4 nm at 450 $^oC$. James Proscia and Gordon [18] showed an increase in grain size with increasing deposition temperature for the FTO thin films produced by APCVD technique and it was attributed to the increase in crystallite size.

Fig. 3 shows the XRD patterns of FTO thin films, spin coated and heated at 400 $^oC$ with different dopant concentrations. The FWHM of the peaks are broad which confirm the nanocrystalline nature possessing tetragonal rutile structure for the FTO films and no other phase than $SnO_2$ is found. All the films showed (110) preferred orientation along with (101) and (211) orientations. Film prepared with 1.0 F at.% show three small peaks having (110), (101) and (211) orientations with lesser intensities. As the dopant concentration is increased to 2.5 and 5.0 at.%, the peak intensity and sharpness of these orientations gradually increase with preferred growth along (110) plane. The spin coated films with 7.5 at.% shows the prominent (110) peak with highest intensity. At higher dopant concentrations, 10 and 12.5 at.%, the intensity decreases for all these planes but the preferred orientation is retained along the (110) plane. A similar effect of dopant concentration on the spray deposited FTO thin films was observed by Chitra Agashe [19]. These variations in the diffraction intensity with the dopant concentration may be attributed to the occupation of fluorine atoms at the substitutional oxygen sites. Fantini and Torriani [23] have reported a systematic increase in the intensity for the (110) and (211) reflections, with the increase in fluorine concentration for the pyrolytically sprayed FTO thin films at a substrate temperature 280 °C. The decline in the diffraction peak intensity and sharpness at higher fluorine concentration (above 7.5 at %) implies that higher doping results in deterioration of the crystalline nature of the lattice and crystallinity of the films tending them to loose their crystallite orientations. The lattice constant a, c and c/a ratio are found to decrease with the increase in dopant concentration. For the F/Sn ratio of 7.5 at.% the values of a, c and c/a were calculated as 4.72A°, 3.19A° and 0.675, which are in well agreement with the standard JCPDS data (41 – 1445).

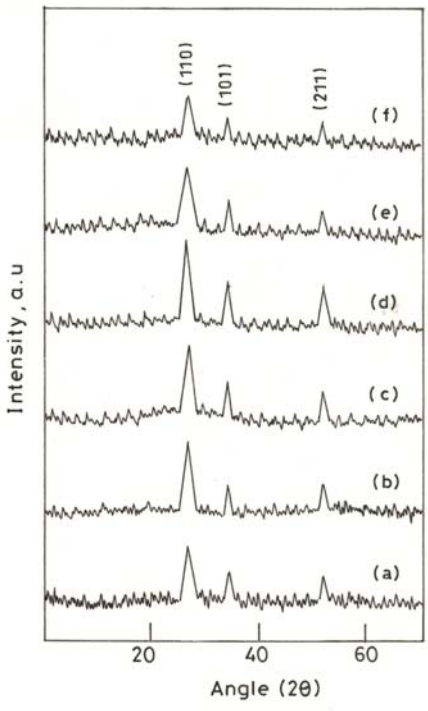


*Fig. 3. XRD pattern of FTO films doped with F/Sn ratios of (a) 1.0, (b) 2.5, (c) 5.0, (d) 7.5, (e)10.5 and (f) 12.5%.*

The variation of grain size with different dopant concentrations is shown in Fig. 4a, which indicates a gradual increase up to F/Sn ratio of 7.5 at.% and then the grain size decreases gradually. The increase in grain size up to the doping level 7.5 at.% is due to the heterogeneous nucleation. At higher dopant concentration perhaps the deterioration of the crystal lattice may be the perturbing factor for the grain growth, which results in smaller crystallites or agreegates of crystallites. The average grain size was found to vary between 3.8 nm and 5.7 nm for the entire range of dopant concentration and a maximum value of 5.7 nm was observed at the optimum doping level F/Sn ratio 7.5 at.%.

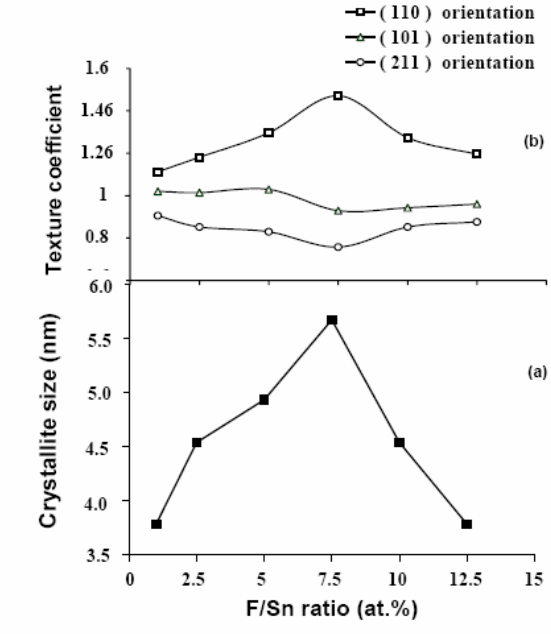


*Fig. 4. Variation of (a) grain size and (b) texture coefficient t with different F/Sn ratios.*

The texture coefficients, TC(110), TC(101) and TC(211), for the three prominent orientations (110), (101) and (211) were calculated from the XRD data and their variation with dopant concentrations are shown in Fig. 4 b. From the figure it is seen that TC(110) increases initially with doping, becomes maximum and then reduces for doping levels more than the optimum level F/Sn ratio of 7.5 at.%. The TC(110) reduces beyond the optimum doping level (7.5 at.%) probably because the heavy doping makes it difficult to form a critical nucleus for development and so the specific interaction of the nucleus with the substrate surface may be reduced, which in turn reduces the grain concentration at the preferred orientation and leads to a deterioration effect on all the planes, at higher doping level.

### 3.2. Electrical properties variation with F-dopant concentration

Variation of resistivity with dopant concentrations for the FTO thin films, heat treated at 375 $^{o}$C, 400 $^{o}$C and 425 $^{o}$C was studied and presented in Fig.5a. It is evident that, resistivity decreases with the increase in dopant concentration and reaches a minimum at the optimum doping level of 7.5 at.%. Above this optimum level, resistivity gradually increases with the increase in F/Sn ratio. The minimum value of sheet resistance ($R_{sh}$) and resistivity ($\rho$) is obtained for the FTO thin film doped with F/Sn ratio 7.5 at.%, and the values correspond to 40 $\Omega$/square and $7.4 \times 10^{-3}$ $\Omega$ cm respectively. These results are in good agreement with the resistivity values of about $6 \times 10^{-3}$ $\Omega$ cm reported, for the spray deposited FTO thin films doped with 1.3 wt. % of $NH_4F$ [24]. Addition of group VII element fluorine in substitution for oxygen or interstitial into the $SnO_2$ structure causes a decrease in resistivity and gives rise to n-type conductivity, which depends on stoichiometric deviation and doping effect. The doping effect is due to a controlled valance mechanism by the controlled valance oxide (FTO) $Sn^{4+}$ $e_x$ $O^{2-}_{(2-x)}$ $F^{-}_{x}$ , in which the contribution of oxygen vacancies to the n-type conductivity is very less. Moreover mobility of free carriers in FTO thin films is found to depend on the nature and concentration of the dopant because fluorine provides shallow donor states [25].

The decrease in resistivity up to 7.5 at.% is due to the increase in the free carrier concentration caused by the exact replacement of more number of oxygen atoms by substitutional fluorine atoms in the lattice under the conditions of relatively lower or moderate doping levels. The increase in carrier mobility is attributed to both grain size increases and the presence of dopant atoms at the grain boundaries [23]. An increase in resistivity with the gradual increase in dopant concentration above this optimum level could be mainly attributed to the reduction in the number of charge carriers as a result of increased lattice disorder and additionally due to the reduction of carrier mobility caused by the dominant grain boundary scattering. This can also be explained on the basis of ionized impurity scattering mechanism, that is observed in an ionic lattice such as $SnO_2$ possess. If the oxygen vacancies are filled with fluorine atoms (FTO structure) then these vacancies may act as strong scattering centers, which will disturb the free motion of electrons, thereby reducing the carrier mobility values at higher F doping levels [12].

The dependence of carrier concentration (n) on the F doping is shown in Fig. 5b. The n value, $1.2 \times 10^{20}$ $cm^{-3}$, observed for the 1 at.% doped film increased to $4.7 \times 10^{20}$ $cm^{-3}$ for the films doped with 7.5 at.% F and then reduced. The variation of mobility ($\mu$) with F doping is given in Fig. 5c. The low mobility (4.1 $cm^2$ $V^{-1}$ $s^{-1}$) value at a low F doping (1.0 at.%) significantly increased to a higher value (17.2 $cm^2$ $V^{-1}s^{-1}$) at higher F doping value (7.5 at.%) and then shows a decreasing trend on further increasing the F doping concentration to 12.5 at.%. Under such conditions, the resistivity of the presently prepared $SnO_2$:F films is

mainly governed by the carrier concentration and mobility which are directly influenced by F doping concentration. This suggests that, for the spin coated $SnO_2$:F films studied here, grain boundary scattering is the only scattering mechanism influenced by the F dopants in the $SnO_2$:F films with nanocrystalline nature with crystallite size (3-6 nm).

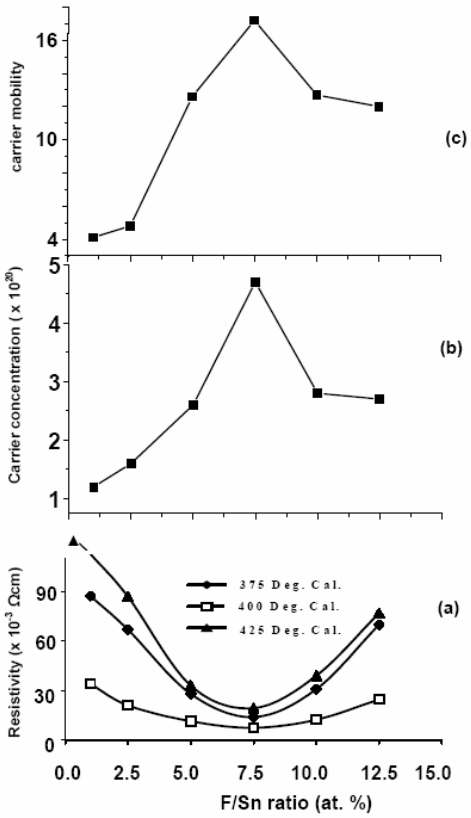


*Fig. 5. Variation of (a) resistivity, (b) carrier concentration and (c) carrier mobility with F dopant concentrations of SnO2:F thin films.*

### 3.3. Optical properties of $SnO_2$:F films

The optical transmittance spectra of FTO thin films spin coated on glass substrates at different dopant concentrations are shown in Fig. 6. For all the films coated at different doping level, a sharp fall in the transmittance is observed near the UV region, which is caused by the fundamental light absorption. Transmittance increased with F doping and the film coated with 7.5 at.% showed the highest optical transmittance. These observations are in good agreement with the reported optical transmittance values for the $SnO_2$:F films prepared by different techniques [26]. A maximum transmittance value of about 94 % (at 550 nm) was observed for the $SnO_2$:F film doped with 7.5 at.% F, which can be attributed to the high carrier density, low scattering and thickness uniformity of the film due to its smooth surface. The average transmittance (in the wavelength region 300 nm to 700 nm) observed was about 86% for the films coated with 7.5 at.% F. These values agree well with the transmittance value of 80-90 % reported by Fang and Chang [27] for their $SnO_2$:F films prepared by chemical vapor deposition route. The decrease in transmittance with the increasing dopant concentration may be due to increased clustering of particles, decrease in carrier density and increase in surface roughness of the film. These phenomena invariably promote the diffused as well as multiple reflections at the surface thereby increasing the absorption nature of the highly doped $SnO_2$:F films in the visible region of solar spectrum [26]. From Fig.6 it is also observed that the optical absorption edge gets shifted to high-energy side with increasing F doping upto 7.5 at.%, indicating an enlarged optical band gap by F doping regardless of crystallinity. The variation of extinction coefficient ($k_f$) with wavelength was calculated for the films with different F dopant concentration. The film doped with 7.5 at.% F shows a low value of extinction coefficient, about $0.1 \times 10^{-4}$, in the wavelength region 375 – 700 nm and the variation is less than $0.5\times10^{-4}$ for all dopant concentrations; these values are the same as that reported for flash evaporated $SnO_2$ films [24]. This may be attributed to the high carrier density and high transmittance of the film in this region owing to its very smooth surface and uniform grain size distribution as observed by SEM and AFM pictures discussed in section 3.4. The variation of refractive index ($n_f$) in the wavelength region 375 to 700 nm for the FTO thin films of nearly the same thickness of about 350 nm was calculated. In the visible region, the refractive indices are almost constant for all the films. The refractive index value at 500 nm is maximum of about 1.97 for the 7.5% F doped films and for other films they are less. This is good in agreement with the reported values of Shanthi et al. [28]. The low value of refractive index may be attributed to the lower density of $SnO_2$:F films as suggested by Elangovan and Ramamurthi [29]. $SnO_2$:F thin films are finding application as n-type layer for silicon based solar cell fabrication and it is necessary to evaluate its opto-electronic performance, by calculating the figure of merit $\phi_{TC}$ for TCO films. It was calculated using the relation $\phi_{TC} = T^{10} / R_{sh}$ [30] in the visible region, where T is the transmittance and $R_{sh}$ is the sheet resistance. $\phi_{TC}$ of the FTO thin films with different dopant concentration viz., F/Sn ratio 5, 7.5 and 10 at.% showed an average maximum value of 0.014 $(\Omega/sq)^{-1}$ at $\lambda$ = 550 nm for the 7.5 at % doping through out the visible region. This value is in very good agreement with the value of 0.031 $(\Omega/sq)^{-1}$ reported by Fukano and Motohino [30] for thin $SnO_2$:F films prepared by intermittent spray pyrolysis route. The $\phi_{TC}$ values are very low, 0.006 and 0.001 $(\Omega/sq)^{-1}$ for the 5 and 10 F at % doped films respectively. From the optical transmission spectra in the UV-Vis region, the absorption coefficient ($\alpha$) at different wavelengths can be calculated [31] from the expression $\alpha = \frac{1}{t}\ln\left(\frac{1}{T}\right)$ where T is the transmission at different wavelengths and t is the film thickness. The absorption coefficient for $SnO_2$: F films are high about $10^4$ $cm^{-1}$ in the studied spectral region. The

optical band gap energy (Eg) proportional to absorption coefficient (α), can be derived from the following equation for TCO films:

$$\alpha = \frac{K\left(h\nu - E_g\right)^{\frac{n}{2}}}{h\nu} \quad (1)$$

*K* is a constant; n is equal to 1 for a direct optical transmission. The direct band gap value can be found out from a plot of $(\alpha h\nu)^2$ against photon energy (hν ) in which the tangent intercepting the photon energy axis gives the band gap energy. The inset of Fig.6 gives a typical plot which yields a band gap value of 3.85 eV allowed direct transition in the 7.5 at.% F doped $SnO_2$ film. The observed band gap values, 3.41, 3.55, 3.60, 3.85,3.75 and 3.45 eV for the F/Sn ratios of 1, 2.5, 5.0, 7.5, 10.0, 12.5 % respectively are shown in Fig. 8. In the case of undoped/films $SnO_2$, the band gap value is about 3.41 eV and the same value is observed for 1 at.% doping concentration. Then, it increased to a maximum of 3.85 eV for 7.5 at.% doped film and then decreased to 3.45 eV for further higher doping to 12.5%. Such an increment in the direct band gap value of $SnO_2$ films by doping with fluorine may be attributed to Burstein-Moss effect [32] which shows an increase in the band gap values of semiconductor films due to heavy doping. The reason for this could be that the allowed states near the bottom of the conduction band are occupied to rather high levels and that the allowed transition from the valence band would have correspondingly higher energies than the forbidden energy gap. Shanthi et al [28] have reported a large Moss – Burstein shift in the absorption edge ranging from 4.35 to 4.40 eV, for their spray deposited FTO thin films.

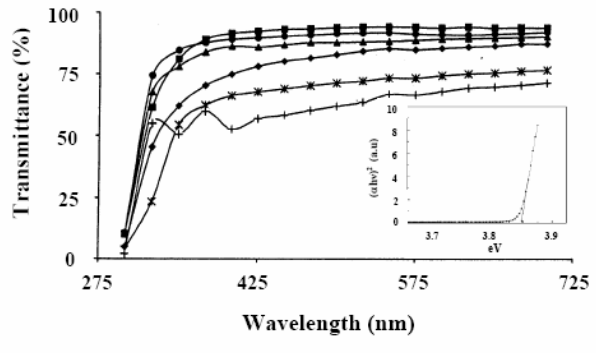


*Fig. 6. Transmission spectra of FTO films corresponding to F dopant concentrations of 1% ( ♦ ), 2.5% ( ▲ ), 5.0% (● ), 7.5% (■ ), 10.0% ( x ) , and 12.5% (+).*

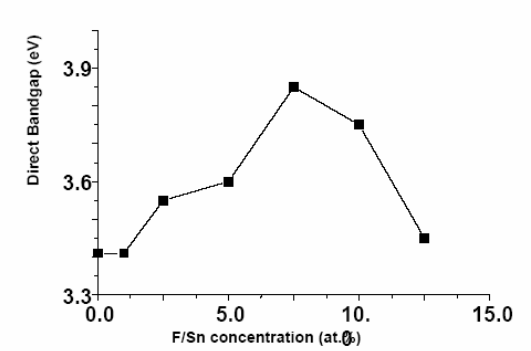


*Fig. 7. Band gap dependence on the F/Sn% of FTO films.*

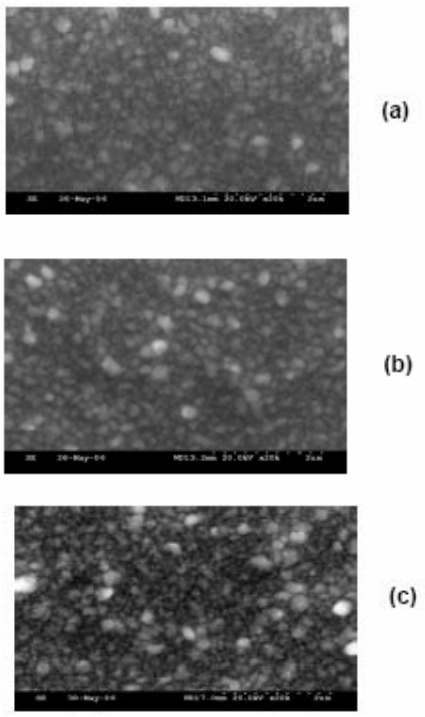


*Fig. 8. SEM images of FTO films prepared at at 400 °C with (a) 2.5% (b) 7.5% and (c) 12.5% F.*

### 3.4. Surface morphological studies

The SEM and AFM images of sol-gel spin coated $SnO_2$:F films deposited with different doping concentrations of 2.5 %, 7.5 % and 12.5 % F are shown in Fig.9. Many crystalline island microstructures embedded with larger grains are seen in Fig.9a, observed on the film surface doped with 2.5 at.% F. As the doping concentration increases to 7.5%, the film becomes closely packed grains of uniform size are seen as in Fig. 9b. On increasing the F doping to 12.5 at.%, the surface shows non-uniform distribution of micrograins and aggregates as observed in Fig. 9c.

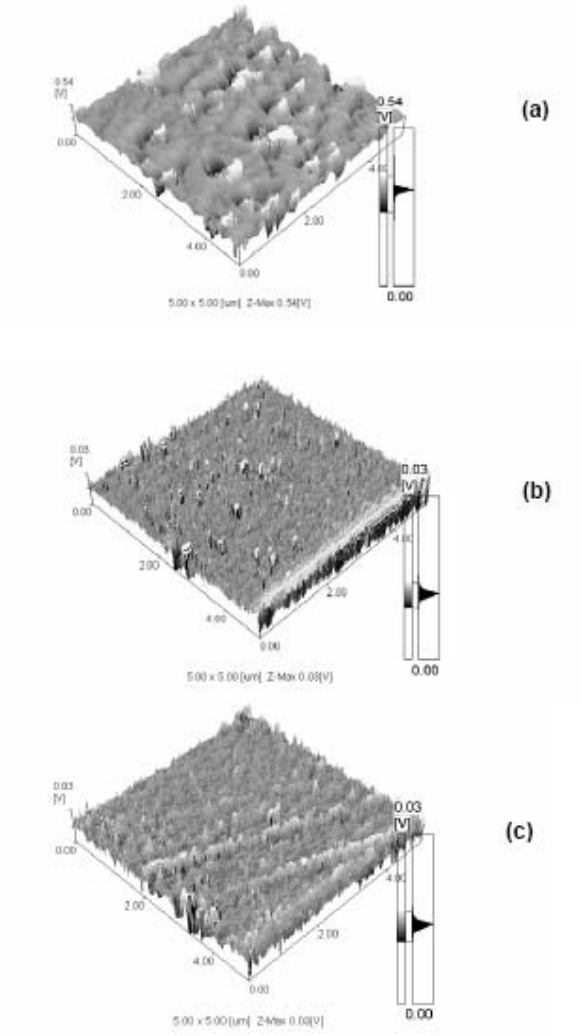


*Fig. 9. AFM picture of $SnO_2$:F films doped with (a) 2.5% F (b) 7.5% and (c) 12.5%.*

The surface topography of $SnO_2$: F films are shown in Fig. 10 a-c for different F doping of 2.5%, 7.5% and 12.5% respectively. The surface morphology of the 7.5 at.% F doped film is found to be more uniform and dense compared to other doped films. The surface roughness is found to increase with F doping concentration from 1% to 12.5%. The root mean square (RMS) roughness of the representative $SnO_2$:F films doped with 2.5, 7.5 and 12.5 % F are about 12, 21.4 and 30.1 nm respectively.

These surface morphologies predict that even though the F doping concentration is varied widely, the surface uniformity is maintained without much deterioration. This is the salient feature of the $SnO_2$:F films developed by the spin coating unit.

## 4. Conclusions

The present studies demonstrate that device quality FTO thin films could be deposited by spin coating with an optimum of 8 number of coating. The results indicate that FTO thin films with the following optoelectronic properties, an average transmittance of 86 %, low electrical resistivity of $7.4 \times 10^{-3}$ Ω-cm and a large band gap of 3.85 eV could be achieved by the sol-gel spin coating technique with an optimum level F/Sn ratio of 7.5 at.%. The surface uniformity is excellent which makes it useful for antireflection coatings and in the development of oxide based solar cells.

## References

[1] N. Amin, T. Isaka, A. Yamada, M. Konagai, Sol. Energy Mater. Sol. Cells **67,** 195 (2001).
[2] S. Iijima, Nature **354**, 56(1991).
[3] W. Han, S. Fan, Q. Li, Y. Hi, Science **277**, 1287 (1997).
[4] H. Dal, E. W. Wong, Y.Z. Lu, S. Fan, C.M. Lieber, Nature **375**, 796 (1995).
[5] X. L. Chen, J. Y. Li, Y. G. Cao, Y.C. Lan, H. Li, M. He, C. Y. Wang, Z. Zhang, Z. Y. Qiao, Adv. Mater. **12,** 1432 (2000).
[6] J. Y. Li, X. L. Chen, Z. Y. Qiao, Y. G. Cao, Y. C. Lan, J. Cryst. Growth **213**, 408 (2000).
[7] G. S. Cheng, L. D. Zhang, Y. Zhu, G. T. Fei, L. Li, C. M. Mo, Y. Q. Yong, Appl. Phys. Lett. **75**, 2455 (1999).
[8] H. J. Dai, E. W. Wong, Y. Z. Lu, S. S. Fan, C. M. Lieber, Nature **375**, 767 (1995).
[9] E. W. Wong, B. W. Maynor, L. D. Burns, C. M. Lieber, Chem. Mater. **8**, 2041 (1996).
[10] C. H. Liang, G. W. Meng, L. D. Zhang, Y. C. Wu, Z. Cui, Chem. Phys. Lett. **329**, 323 (2000).
[11] Y. C. Choi, W. S. Kim, Y. S. Park, S. M. Lee, D. J. Bae, Y. H. Lee, G. S. Park, W. B. Choi, N. S. Lee, J. M. Kim, Adv. Mater. **12**, 746 (2000).
[12] I. Hamberg, C. G. Granqvist, J. Appl. Phys. **60**, R 123 (1986).
[13] P. Nunes, E. Forturato, R. Martins, Int. J. Inorg. Mater. **3,** 1125 (2001).
[14] J. H. Lee, B. O. Park, Thin solid films **426,** 94 (2003).
[15] J. P. Zheng, H. S. Kwok, Appl. Phys. Lett. **63**, 1 (1993).
[16] F. B. Ellis, J. Houghton, J. Mater. Res. **4**, 863 (1996).
[17] T. Ishida, O. Tabata, J. I. Park, S. H. Shin, H. Magara, S. Tamura, S. Mochizuk, T. Mihara, Thin Solid Films **281-282,** 228 (1996).
[18] J. Proscia, R. G. Gordon, Thin Solid Films **214**, 175 (1992).
[19] Chitra Agashe, M. G. Takwale, B. R. Marathe, V.G. Bhide, Solar Energy Materials **17**, 99 (1998).
[20] C. D. Feng, Y. Shimizu, M. Egashira, J. Electrochem. Soc. **141**, 220 (1994).
[21] C. J. Brinker, G. W. Scherer, Sol-Gel Science, The Physics and Chemistry of Sol-Gel Processing, Academic Press, San Diego (1990).
[22] S. S. Park, H. Zheng, J. D. Mackenzie, Mater. Lett. **22**, 175 (1995).
[23] M. Fantini, I. Torriani, Thin Solid Films **138**, 255 (1986).
[24] J. C. Manifacier, Thin Solid Films **90**, 297 (1982).
[25] K. L. Chopra, S. Major, D. K. Pandya, Thin Solid

Films **102**, 1(1983).
[26] J. L. Yung, J. W. Ching , Surf. Coat. Technol. **88**, 239 (1996).
[27] T. H. Fang, W. J. Chang, Appl. Surf. Sci. **220,** 175 (2003).
[28] S. Shanthi, C. Subramanian, P. Ramasamy, Cryst. Res. Technol. **34**, 1037 (1999).
[29] E. Elagovan, K. Ramamurthi, J. Optoelectron. Adv. Mater. **5**, 45 (2003).
[30] T. Fukano, T. Motohino, Sol. Energy Mater. Sol. Cells **82**, 567 (2004).
[31] M. J. Alam, D. C. Cameron, Surf. Coat. Technol. **142-144**, 776 (2001).
[32] B. E. Sevnelius, K. F. Beggren, Z. C. Jin, I. Hambarg, C. G. Granqvist, Phys. Rev. B **37**, 10244 (1988).

*Corresponding author: jayam54@yahoo.com